Published by IOP Publishing for Sissa Medialab

Received: *August 5, 2024*
Revised: *November 25, 2024*
Accepted: *January 10, 2025*
Published: *February 7, 2025*

Studies of the geometric effect for gaseous X-ray polarimetry

Jiechen Jiang,[a,b] **Yang Jiao**,[a,b,c] **Weichun Jiang**,[a,b,*] **Xiaohua Liu**,[a,b] **Yuanyuan Du**,[a,b] **Hong Li**,[a,b] **Qiong Wu**,[a,b] **Xiaojing Liu**,[a,b] **Liang Sun**,[a,b] **Jiawei Yang**,[a,b] **Yupeng Xu**,[a,b,c] **Huilin He**,[a,b,c] **Hua Feng**,[a,b] **Congzhan Liu**,[a,b] **Hangyu Chen**,[a,b,c] **Zipeng Song**[a,b,c] **and Yongqi Zhao**[a,b]

[a] *Institute of High Energy Physics, Chinese Academy of Sciences (CAS), Beijing 100049, China*
[b] *Key Laboratory of Particle Astrophysics, Chinese Academy of Sciences (CAS), Beijing 100049, China*
[c] *University of Chinese Academy of Sciences, Beijing 100049, China*

E-mail: jiangwc@ihep.ac.cn

Abstract: The geometric effect is an intrinsic response of gaseous X-ray polarimetry, which exhibits some sharp peaks with a fixed period angle on modulation curves, especially in observations of unpolarized sources, resulting in spurious modulation and a deviation of polarization detection. We construct a simulation framework to study the origin of the geometric effect and evaluate the impact on the performance of the polarimetry. The modulation curves from the simulation are consistent with measurements while focusing on the geometric effect. The studies show that the geometric effect is from the photoelectrons generated close to multiplier stages, a more significant geometric effect with a deeper depth of the photoelectric impact point. The effect was characterized by a diffusion coefficient related to photoelectric drift height to quantify the geometric effect. From the simulation results, choosing smaller detector units could suppress the effect, and the size of the detector unit is 1.25 times larger than the diffusion coefficient related to an observable geometric effect. In addition, the relative contribution to the effect is approximately 65% for the GEM hole pitch and 35% for the readout pitch. This study provides a reference for detection unit optimization and the threshold setting of fired pixels in observations.

Keywords: X-ray detectors and telescopes; Gaseous detectors; Software architectures (event data models, frameworks and databases)

*Corresponding author.

https://doi.org/10.1088/1748-0221/20/02/P02007

Contents

1 Introduction

Gaseous detectors are widely used in X-ray polarimetry [1–4]. Two main types among them at present; one is the Gas Pixel Detector (GPD) [5], and the other is the Time Projection Chamber (TPC) [6]. 2-D projection images of photoelectric tracks can be obtained for both of them. The difference is that 2-D coordinates are pixel positions for the GPD polarimetry, while one of the coordinates is the arrival time of signal for the TPC polarimetry. The GPD polarimetry has better position resolution and can image X-ray sources directly, while the TPC polarimetry could have a greater detector efficiency. Whatever types in X-ray observation, the geometric effect is observed on the modulation curves for the events with fewer fired pixels. The geometric effect means the modulation curves exhibit sharp peaks with a fixed angle period, which corresponds to the spatial distribution pattern of detector units, such as the GPD polarimetry; a 60° periodicity shows on the modulation curve, which reflects the spatial distribution with hexagonal pattern for detector units. [7] The geometric effect distorts the distribution of modulation curves, especially in unpolarized sources observation; the periodic peaks are distinct, resulting in a spurious modulation and deviation of polarization detection. Although [7] found the geometry effect in the GPD polarimetry, the origin and limitation of the effect need to be further studied, and the influence on the polarization performance could not be quantified and effectively evaluated. Therefore, we constructed a simulation framework and chose the GPD polarimetry as an object in this study to pursue these unclear points. The glossary defined in this paper is shown in Tab 1.

Table 1. The glossary defined in this paper.

Detector unit	A unit that consists of a single GEM hole and a readout pixel, both featuring the same pitch.
Size of the detector unit	the pitch of the detector unit.
Contribution ratio	The proportion of the pitch of the GEM hole and pitch of the readout pixel, relative to the size of the detector unit or the reduced detector unit.
Reduced detector unit	Equivalent detection unit, encompassing a single GEM hole and a readout pixel with different pitch.

2025 JINST 20 P02007

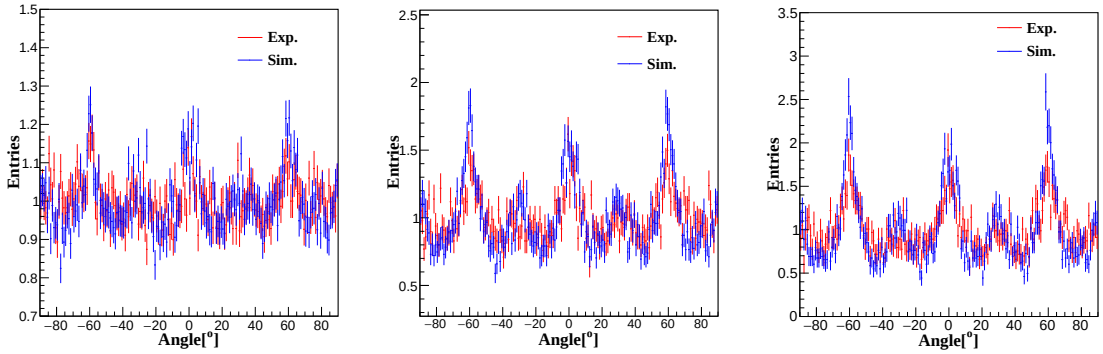

Figure 1. The modulation curves obtained from simulation and experiments in response to unpolarized X-rays at 4.5 keV, the number of events is 100,000 for them. The left panel is the modulation curve without event selection, and the middle and right panel is 20 % and 10 % events with fewer fired pixels, respectively.

2 Validation of simulation framework

The geometric effect is related to the size and spatial distribution of detector units within gaseous X-ray polarimetry, which indicates the effect confirmed after the structure of detector units is determined. Although the effect could be regarded as background and calibrated, it will increase too much time in the calibration procedure. In general, the calibration period is several months for each polarimeter. [8] To reduce the calibration time and suppress the geometric effect simultaneously, studies of the origin and limitations of the effect are necessary. We refer to [9] and construct a simulation framework to focus on the studies of the effect. Although [9, 10] verified the feasibility of the framework applied in the X-ray polarimetry, the geometric effect is not mentioned. Therefore, we compare the effect between simulation and measurements in the first.

The parameters of the detectors are in [11], the only difference is that the hole pitch and hole diameter of the Gas Electron Multiplier (GEM) are 100 µm and 50 µm, respectively. The figure shows modulation curves obtained from simulation and measurements. The incident energy is 4.5 keV with unpolarized X-rays; the emission direction of photoelectrons is reconstructed by the standard algorithm [12]. The periodic peaks are observed in figure 1; the peak values reflect the magnitude of the influence of geometric effects. Two different patterns of peaks with 60° period are observed in the figure, one is (−60°, 0°, 60°), the other is (−90° (or 90°), −30°, 30°). These two patterns correspond to the first (60° spatial distribution) and second (30° spatial distribution) circular detector units surrounding the photoelectric impact point, as presentation in the left panel of figure 3. The detector units with the same spatial angles overlap on the modulation curve, resulting in more visible peaks for the first pattern. The modulation curves from the simulation are consistent with measurements with different event selection rates, indicating that the geometric effect could be studied with the simulation framework. The peak values in the simulation are a little larger than measurements if focused on this region. The reason is that the detector units are the same in the simulation, whereas non-uniformity exists among them during production in reality [13], resulting in a relatively smooth peak trend. In figure 1, the 20° period pattern is not apparent, suggesting that the geometric effect could be eliminated if the threshold for activated pixels is set to 37, which corresponds to the number of pixels comprising the first three circular detector units; however, the geometric effect also exists in the left panel of

2025 JINST 20 P02007

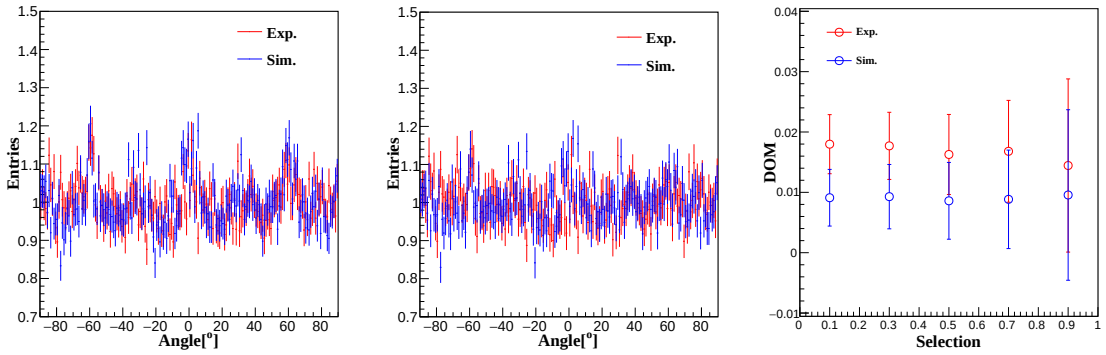

Figure 2. The left is the events with the number of fired pixels above 37; the middle is the curves after removing 10% events with fewer fired pixels; the right is the DOM with different event selection rates; the X-axis means different cutting event rates with fewer fired pixels.

figure 2. The middle panel of figure 2 shows the modulation curves after removing 10% of events with fewer fired pixels. The periodic peaks are not distinct, which means the geometric effect could be suppressed after removing those events with fewer fired pixels. With the threshold increase, the degree of modulation (DOM) changes a little, as shown in the right panel of figure 2, which indicates that the polarization performance could not be affected while eradicating the geometric effect.

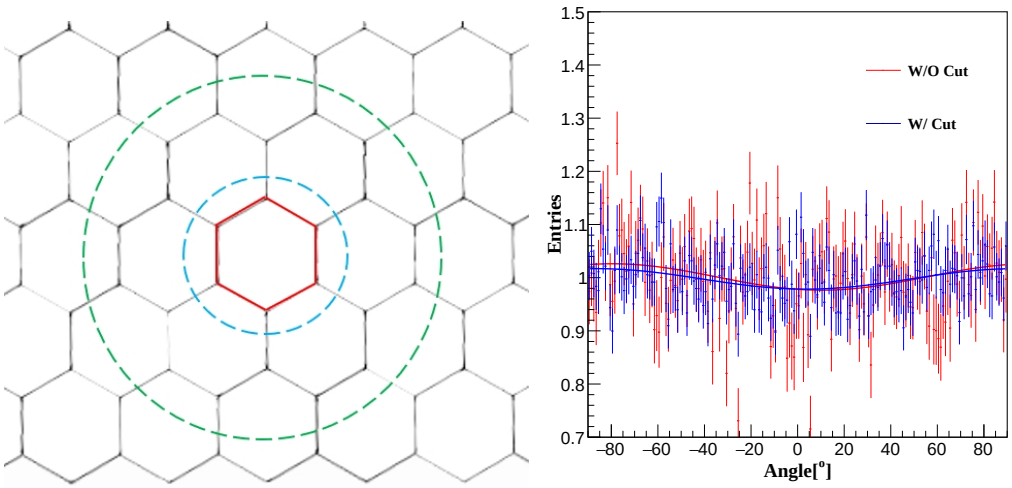

Figure 3. The left panel presents a diagram of the circular region, with the blue and green circles encompassing the first and second annuli surrounding the detector unit. Right panel shows the data after removal of 10 % events with fewer fired pixels (blue) and the subtraction of the simulated distribution with geometric effects (red), the DOM is $1.87 \pm 0.46\%$ and $2.47 \pm 0.64\%$, the polarization angle is $-79.6° \pm 7.43°$ and $-87.0° \pm 7.09°$.

Based on the discussion above, the geometric effect could be suppressed by removing the events with fewer fired pixels; however, this method results in a reduced event rate. An alternative approach to suppress the effect involved subtracting the distribution from the simulations.The red curves in figure 3 represent the data after this subtraction from the simulated modulation curves in the left plot of figure 1, while the blue curves denote the data obtained after the removal of 10% of the events

2025 JINST 20 P02007

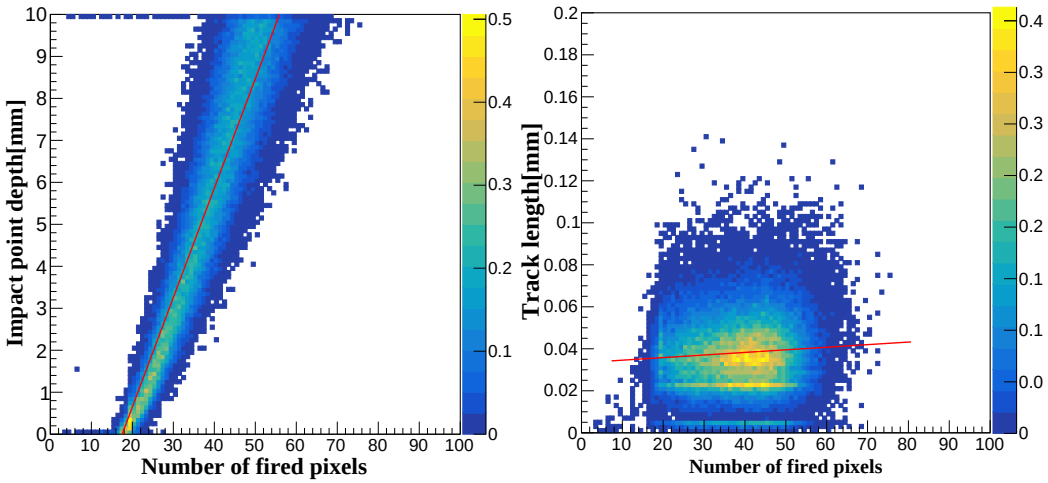

Figure 4. The relationship between the number of fired pixels and the depth of the photoelectric impact point (left) or track length (right), the track length is defined as the length of the photoelectric trajectories projected onto the X-Y plane. The incident energy is 2 keV, and the size of the detector unit is 50 µm (pitch of GEM holes and readout pixels is 50 µm).

with fewer fired pixels. The fitting curves exhibit consistent DOM and polarization angles within the statistical uncertainties for both cases, suggesting that the geometric effects could be removed from the actual data, potentially shortening the calibration time without affecting accuracy. For the polarized X-rays, the height of the geometrical peaks may vary, with the peak heights reaching their maximum and minimum values at an angle difference of 0° and 30° with respect to the polarization vector and the geometrical angle of the detector unit.

In this simulation, 100,000 events are considered, with a statistical uncertainty of 0.0044. Notably, the required number of photons is more than an order of magnitude higher in the measurements to achieve a reliable minimum detectable polarization at this level. The photoelectric electrons are reconstructed using the first step of algorithm in the following study [12], causing the geometric effect has more impact on the GPD extension into lower X-ray energies and the algorithm is more accurate in this energy band [7].

3 Origin of the geometric effect

Based on the discussion in section 2, events with relatively fewer fired pixels lead to the geometric effect. These events are mainly from two situations: one is short photoelectric tracks, and the other is photoelectrons generated close to multiplier stages. For the latter one, eq. 3.1 gives diffusion coefficients at different drift heights of photoelectrons,

$$D_t = D_T \times \sqrt{d} \tag{3.1}$$

where D_T is the gaseous diffusion coefficients, d is the drift height of photoelectrons, and the diffusion coefficients D_t decrease with drift heights d decrease, resulting in events with relatively fewer fired pixels. Figure 4 gives the relationship between fired pixels and the depth of photoelectric impact points or track length. The number of fired pixels increases with a higher drift height of photoelectrons, and

2025 JINST 20 P02007

the overall trend is linearity, whereas the right panel shows that the slope value is small. This tendency indicates that the depth of the photoelectric impact point dominates the geometric effect, while the photoelectric track length has little impact. That is to say, the effect changes a little with a variation of incident X-ray energy, and the same threshold of fired pixels could be applied in polarization detection. The geometric effect from the photoelectrons generated with different impact depths is compared to check this point. Figure 5 left is the distribution of the photoelectric drift height at 2 keV X-rays, and we divided it into five bands. Figure 5 right gives the modulation curves corresponding to each band shown on the left. The periodic peaks are distinct in the first band and fade out with an increase in drift height, which illustrates that the geometric effect originates from the photoelectrons generated close to multiplier stages as the structure of detection units is determined.

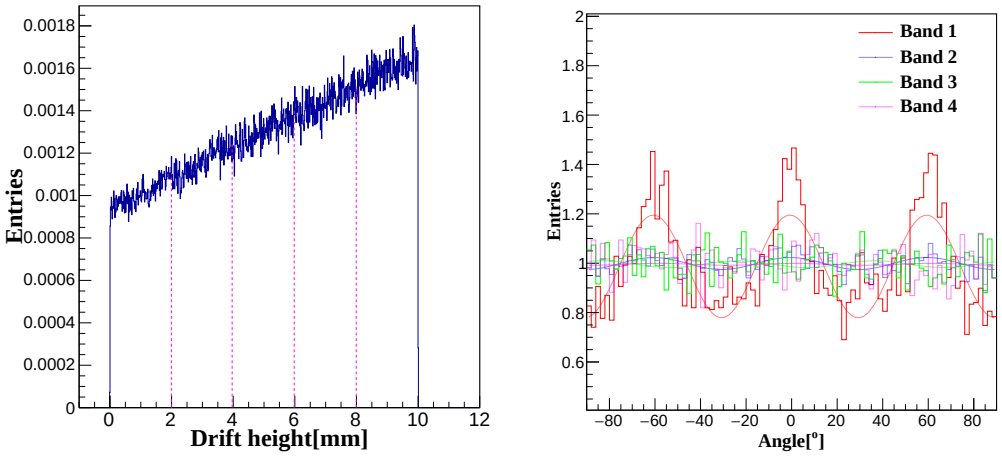

Figure 5. The left is the distribution of the drift height where photoelectrons generation and the X-axis is the distance away from the GEM; the region is divided into 5 bands, number 1∼5 from left to right. The right is the modulation curve corresponding to the events in different bands shown on the left, the fitting curves are from the eq. 4.1.

4 Optimization of detector units

Although photoelectric drift height dominates in the geometric effect from section 3, the condition of the observable geometric effect is uncertain, and the influence could not be evaluated for different detector units. Therefore, these two points are focused and studied in this section.

In gaseous X-ray polarimetry, the resolution of photoelectric images depends on the size of detector units that consist of multipliers and readout pixels. In general, the hole pitch of multipliers and pixel pitch of readout electrodes are the same [6, 13]; thus, the size of detector units could be characterized by one parameter. Considering that the photoelectric track length has little impact on the geometric effect, we ignore the track length and take into a single point for each event. Two advantages are associated with this simplification. First, it excludes the influence of operating conditions and provides a general evaluation of the geometric effect for the GPD based polarimeters, where the diffusion coefficient and track length are contingent upon the gas type, operating pressure, and temperature. Second, extending the interval of interest to encompass the geometric effect, particularly in regions with lower diffusion coefficients, could potentially amplify this effect to some extent.

2025 JINST 20 P02007

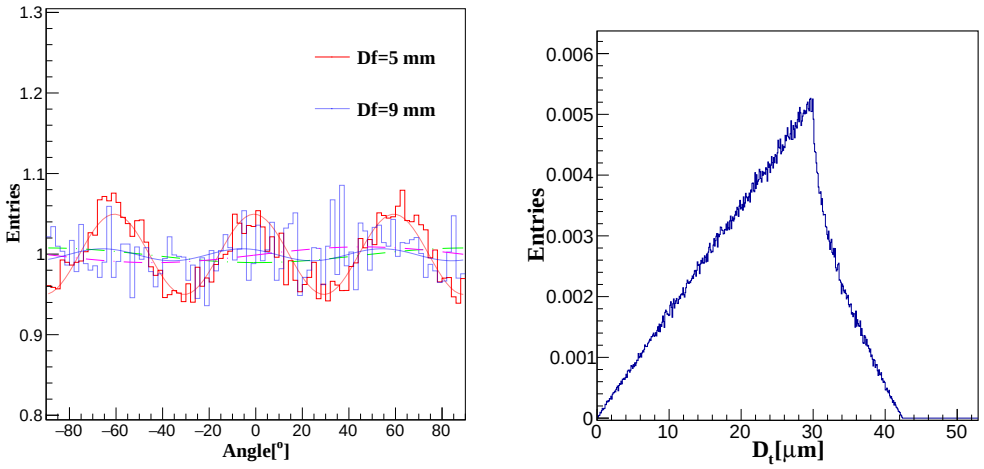

Figure 6. The left is the modulation curves with two different drift height at 9 mm and 5 mm, the pitch of GEM holes and readout pixel is 100 µm and 50 µm with a D_T of 66.5 µm, the mean value of DOM is 0.90 ± 0.20% (pink) and 0.97 ± 0.44% (green) by eq. 4.2, while DOM is 4.98 ± 0.21% (red) and 0.74 ± 0.44% (blue) by eq. 4.1 as drift heights at 9 mm and 5 mm. The right is the sampling distribution of diffusion coefficients in the simulation; the value is the total diffusion coefficients, including drift and transfer region.

Based on the modulation curves in figure 5, the geometric effect is observed only in the first band. In this plot, the fitting function differs slightly from the known formula, which is given by the eq. 4.1,

$$A + B\cos^2(3(\phi - \phi_0)) \tag{4.1}$$

where A and B represent the constant and polarized terms, respectively, and the coefficient value of 3 indicates the number of peaks within the range of 0 to π (a period of 60°) for the GPD. The reason why we introduced the fitting function to model the curves is discussed in the right plot of figure 6. As depicted in the left panel of figure 6, the DOM is comparable between the pink and green fitting curves; however, the peaks are more distinct as the drift height is 5 mm with a smaller fitting value of DOM while comparing to the drift height at 9 mm fitted by eq. 4.2.

$$A + B\cos^2(\phi - \phi_0) \tag{4.2}$$

This situation brings to mistake on the condition where the geometric effect is observed. To qualify the geometric effect, the eq. 4.1 is induced. With the eq. 4.1, the DOM significantly differs in figure 6 and can signify the presence of the geometric effect in the modulation curves.

As discussed above, the geometric effect is from photoelectrons generated with a lower drift height. We use the parameters of drift height to characterize and quantify the geometric effects. From eq. 3.1, the drift height could be converted by diffusion coefficients, and the relationship between diffusion coefficients and the size of detector units is studied. If the diffusion coefficients and distribution of the impact point are known, and the relationship between them and fired pixels are obtained, e.g., the left panel in figure 4 and figure 5. The effective event rate and threshold of fired pixels could be estimated. Diffusion coefficients are uniformly distributed with samples ranging from 0 to 30 µm in both the drift region and transfer regions in polarimetry. Although the absorption points in drift

2025 JINST 20 P02007

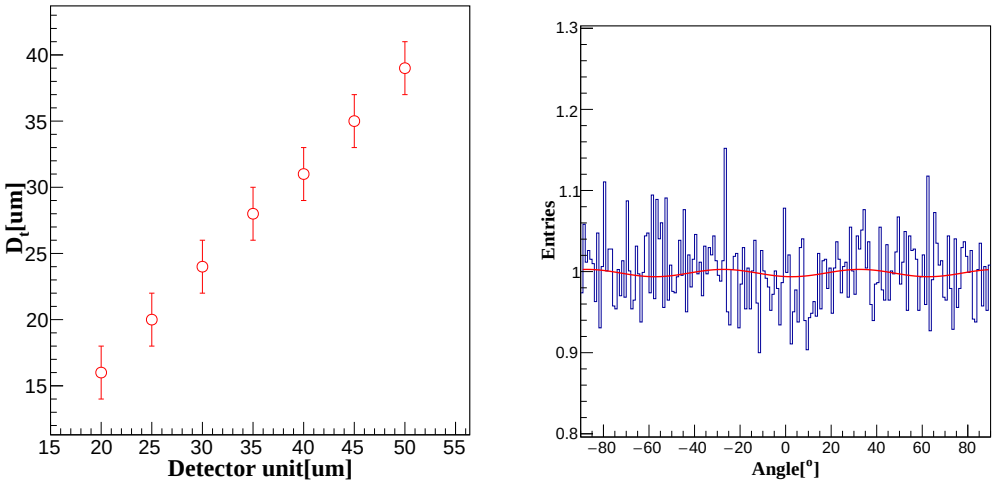

Figure 7. The relationship between detector units and diffusion coefficients where the geometric effect could be suppressed, the experimental error is ±2 µm caused by a judgment deviation where the geometric effect could be observed. Right is the modulation curve as the size of the detector unit is 40 µm, and the diffusion coefficient is 33 µm, the DOM is 0.45 ± 0.44%.

region dominate the diffusion coefficients in reality, choosing this scanning way could quickly find a range of diffusion coefficients where the geometric effect could be observed and decrease sample generation in the simulation. The distribution of diffusion coefficients is given in the right panel of figure 6. The X-axis D_t equals $\sqrt{(D_{\rm dr})^2 + (D_{\rm in})^2}$, where $D_{\rm dr}$ and $D_{\rm in}$ is diffusion coefficients within the drift and induction region, respectively. The relationship between the size of detector units and diffusion coefficients is given in figure 7, the diffusion coefficients are linear with the size of detector units with a linearity coefficient of around 1.25, which means the geometric effect related to a diffusion coefficient of 40 µm could be suppressed as the size of the detector unit is 50 µm. The relationship shown in figure 7 is a key to evaluating and quantifying the influence of the geometric effect. Figure 7 left shows the experimental error bars of each diffusion coefficient caused by a judgment deviation where the geometric effect is observed. The modulation curves are compared for all boundary values to check whether the range of diffusion coefficient is reasonable. Right panel of figure 7 presents the modulation curve associated with a detector unit size of 40 µm and a diffusion coefficient of 33 µm, and the periodic peaks are not observed.

The discussion above is the same pitch of multiplier holes and readout electrodes within detector units; the units with different pitches are also studied. The diffusion coefficient keeps a fixed value of 56 µm (70 µm for the size of detector unit evaluated from figure 7) here to find their respective contribution to the geometric effect. We scanned different constitutions of pitch values of GEM holes and readout pixels, and the relationship is given in the left panel of figure 8. In this figure, one of the pitch values is 70 µm as the diffusion coefficient is 56 µm, and the ratio is just 1.25, showing a consistent ratio in figure 7. Even though the contribution ratio to the geometric effect is not known prior, the points exhibit a liner trend in the figure 8, thus, eq. 4.3 is induced here to describe the relationship between the detector unit (the reduced detector unit) and the pitch of the GEM holes (or the readout pixel).

$$P_{\rm D} = r_{\rm GEM} \times P_{\rm GEM} + r_{\rm readout} \times P_{\rm readout} \tag{4.3}$$

2025 JINST 20 P02007

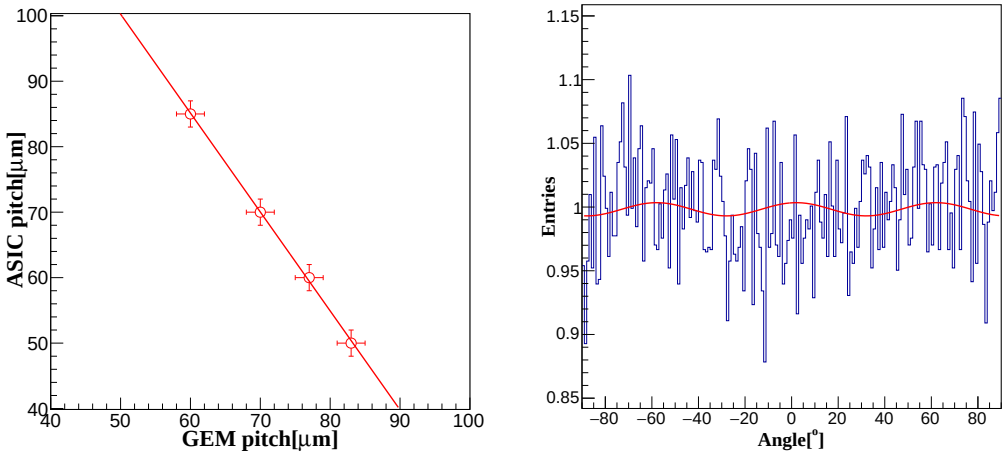

Figure 8. The relationship between the pitch of GEM holes and readout pixels as the diffusion coefficient is 56 μm; the experimental error bar is ±2 μm for them. The right is the modulation curve as the pitch of GEM holes and readout pixel is 100 μm and 50 μm; the diffusion coefficient is 60 μm, the DOM is 0.52 ± 0.44%.

where P_{D} is the size of the detector unit or the reduced detector unit, P_{GEM}, P_{readout} is the pitch of GEM and readout, the r_{GEM} and r_{readout} is the contribution ratio for pitch of GEM and readout, respectively. Based on the definition of the contribution ratio, the sum of the coefficients r_{GEM} and r_{readout} equals 1. For the detector unit, we have $P_{\mathrm{D}} = (r_{\mathrm{GEM}} + r_{\mathrm{readout}}) \times P_{\mathrm{readout}} = P_{\mathrm{GEM}} = P_{\mathrm{readout}}$, given $r_{\mathrm{GEM}} + r_{\mathrm{readout}} = 1$. This implies that the size of the detector unit is independent of the contribution ratio. Regarding the reduced detector unit, the contribution ratio could be obtained by fitting with eq. 4.3, the value of the r_{GEM} and r_{readout} is around 0.65 and 0.35 for the pitch of GEM holes and readout pixels, respectively. Here is an example to check the experimental equation of the reduced detector unit. The pitch of GEM holes and readout pixel is respectively 100 μm and 50 μm, the value of the reduced detector unit is 82.5 μm calculated by the equation, and the value of diffusion coefficient of 66 μm is then obtained. As shown in the right panel of figure 8, the periodic peaks are not observed as the diffusion coefficient is 60 μm, that is to say, the geometric effect is suppressed and less significant for the value of diffusion coefficient of 66 μm even if consider the evaluation deviation of the equation. This result verifies the feasibility of the experimental equation.

5 Conclusion

We focused on the geometric effect in gaseous X-ray polarimetry and chose the GPD polarimetry as a reference in this study. Under the condition of different selection event rates, the geometric effect from the simulation is consistent with measurements in response to unpolarized X-rays at 4.5 keV. With the help of the simulation framework, the geometric effect can be summarized in the following list of characteristics:

- The effect exists in the events with fewer fired pixels; removing these events has little impact on polarization detection.
- As the structure of detector units is confirmed, the depth of photoelectric impact points dominates in the effect, whereas the energy of incident X-ray has little influence.

2025 JINST 20 P02007

- The value of the diffusion coefficient where the effect could be suppressed decreases linearly with a decrease in the size of detector units. The size of detector units is around 1.25 times larger than the diffusion coefficients.
- The modulation factor increases with a decrease in the diffusion coefficient or the size of the detector unit. A higher relative modulation factor can be achieved if the diffusion coefficient at which the effect is suppressed is lower.
- The contribution ratio to the effect is around 65:35 for GEM holes and readout pixels. The size of the reduced detector units could be calculated by the experimental ratio.

Based on these points, the same threshold of fired pixels could be chosen in the observation, and the influence on the geometric effect could be evaluated for detector units with different sizes. This study quantifies the geometric effects by the diffusion coefficient where photoelectron generation and provides a reference for the detection units and the threshold choosing of fired pixels in observations.

Acknowledgments

Thanks to Yusan's group for their support and the 100-m X-ray Test Facility of the Institute of High Energy Physics. This work is supported by the Strategic Priority Program on Space Science, the Chinese Academy of Sciences, Grant No. XDA15020500, XDA15020501, XDA15020501-01, XDA15020501-02 and the CNSA program (D050102).

References

[1] H. Feng et al., *Re-detection and a Possible Time Variation of Soft X-ray Polarisation from the Crab*, *Nature Astron.* **4** (2020) 511 [arXiv:2011.05487].

[2] M.C. Weisskopf et al., *A space-borne X-ray imaging polarimeter*, *Nature Astron.* **7** (2023) 635.

[3] W.B. Iwakiri et al., *Performance of the PRAXyS X-ray Polarimeter*, *Nucl. Instrum. Meth. A* **838** (2016) 89 [arXiv:1610.06677].

[4] R. Gill, M. Kole and J. Granot, *GRB Polarization: A Unique Probe of GRB Physics*, *Galaxies* **9** (2021) 82 [arXiv:2109.03286].

[5] R. Bellazzini et al., *Gas pixel detectors for x-ray polarimetry applications*, *Nucl. Instrum. Meth. A* **560** (2006) 425 [astro-ph/0512242].

[6] J.K. Black et al., *X-ray polarimetry with a micropattern TPC*, *Nucl. Instrum. Meth. A* **581** (2007) 755.

[7] F. Muleri et al., *Spectral and polarimetric characterization of the Gas Pixel Detector filled with dimethyl ether*, *Nucl. Instrum. Meth. A* **620** (2010) 285 [arXiv:1003.6009].

[8] F. Muleri et al., *The IXPE instrument calibration equipment*, *Astropart. Phys.* **136** (2022) 102658 [arXiv:2111.02066].

[9] J. Jiang et al., *A fast simulation model of 2-D photoelectron track images for gaseous X-ray polarimetry*, *Nucl. Instrum. Meth. A* **1050** (2023) 168147.

[10] D.-F. Yi et al., *Star-XP: A simulation framework for Polar-2/ low energy X-ray polarization detector*, *SoftwareX* **25** (2024) 101626.

2025 JINST 20 P02007

[11] H. Li et al., *Assembly and test of the gas pixel detector for X-ray polarimetry*, *Nucl. Instrum. Meth. A* **804** (2015) 155.

[12] R. Bellazzini et al., *Novel gaseous x-ray polarimeter: data analysis and simulation*, *Proc. SPIE* **4843** (2003) 155.

[13] L. Baldini et al., *Design, construction, and test of the Gas Pixel Detectors for the IXPE mission*, *Astropart. Phys.* **133** (2021) 102628 [arXiv:2107.05496].

2025 JINST 20 P02007